Glucose Uptake Inhibition Decreases Expressions of Receptor Activator of Nuclear Factor-kappa B Ligand (RANKL) and Osteocalcin in Osteocytic MLO-Y4-A2 Cells

Ayumu Takeno, Ippei Kanazawa, Masakazu Notsu, Ken-ichiro Tanaka and Toshitsugu Sugimoto

Internal Medicine 1,

Shimane University Faculty of Medicine,

89-1, Enya-cho, Izumo, Shimane 693-8501, Japan

E-mail address: Ayumu Takeno; atakeno@med.shimane-u.ac.jp

Ippei Kanazawa; ippei.k@med.shimane-u.ac.jp

Masakazu Notsu; mnotsu25@med.shimane-u.ac.jp

Ken-ichiro Tanaka; ken1nai@med.shimane-u.ac.jp

Toshitsugu Sugimoto; sugimoto@med.shimane-u.ac.jp

Correspondence and requests for reprints:

Ippei Kanazawa

Internal Medicine 1, Shimane University Faculty of Medicine

89-1, Enya-cho, Izumo, Shimane 693-8501, Japan

Phone: +81-853-20-2183, FAX: +81-853-23-8650

E-mail: ippei.k@med.shimane-u.ac.jp

Running Head

Roles of glucose uptake in osteocytes for bone metabolism

Abstract

Bone and glucose metabolism are closely associated with each other. Both osteoblast and osteoclast functions are important for the action of osteocalcin, which plays pivotal roles as an endocrine hormone regulating glucose metabolism. However, it is unknown whether osteocytes are involved in the interaction between bone and glucose metabolism. We used MLO-Y4-A2, a murine long bone-derived osteocytic cell line, to investigate effects of glucose uptake inhibition on expressions of osteocalcin and bone-remodeling modulators in osteocytes. We found that glucose transporter 1 (GLUT1) is expressed in MLO-Y4-A2 cells and that treatment with phloretin, a GLUT inhibitor, significantly inhibited glucose uptake. Real-time PCR and western blot showed that phloretin significantly and dose-dependently decreased the expressions of RANKL and osteocalcin, whereas osteoprotegerin or sclerostin was not affected. Moreover, phloretin activated AMP-activated protein kinase (AMPK), an intracellular energy sensor. Coincubation of ara-A, an AMPK inhibitor, with phloretin canceled the phloretin-induced decrease in osteocalcin expression, but not RANKL. In contrast, phloretin suppressed phosphorylation of ERK1/2, JNK, and p38 MAPK, and treatments with a p38 inhibitor SB203580 and a MEK inhibitor PD98059, but not a JNK inhibitor SP600125, significantly decreased expressions of RANKL and osteocalcin. These

results indicate that glucose uptake by GLUT1 is required for RANKL and osteocalcin expressions in osteocytes, and that inhibition of glucose uptake decreases their expressions through AMPK, ERK1/2 and p38 MAPK pathways. These findings suggest that lowering glucose uptake into osteocytes may contribute to maintain blood glucose levels by decreasing osteocalcin expression and RANKL-induced bone resorption.

Keywords:

phloretin, osteocyte, GLUT, RANKL, osteocalcin

1. Introduction

Bone is constantly renewed by osteoclasts, the bone resorbing cells, and osteoblasts, the bone forming cells. Osteocytes are the most abundant cells in bone and play pivotal roles in bone remodeling by regulating both osteoblast and osteoclast functions. Receptor activator of nuclear factor-kappa B ligand (RANKL) is an osteoclast differentiating factor which is produced by osteoblastic cells, binds to receptor activator of nuclear factor-kappa B (RANK) on the surface of osteoclasts, and enhances osteoclast differentiation and bone resorption (23). Previous studies showed that osteocytes are the most important source of RANKL to regulate osteoclastogenesis and bone resorption (16). Moreover, osteocytes produce osteoprotegerin (OPG), a decoy receptor for RANKL, and sclerostin, which antagonizes Wnt/beta-catenin signals in osteoblasts and suppresses osteoblast differentiation (1-3).

Recent studies have shown that bone regulates whole body glucose homeostasis through undercarboxylated osteocalcin (ucOCN) (14, 4, 6). Osteocalcin (OCN) is specifically expressed in osteoblast lineages and undergoes γ-carboxylation of glutamyl residues at three positions 17, 21, and 24, which facilitates binding of OCN to hydroxyapatite in bone matrix. Furthermore, osteoclasts are reported to be necessary for the function of ucOCN in glucose metabolism, because acidification is essential for

72 decarboxylation of OCN accumulated in bone matrix (4). When osteoclast-mediated
73 decarboxylation and bone resorption release ucOCN into the circulation, ucOCN
74 promotes proliferation of pancreatic β cells and increases insulin secretion as well as
75 enhances insulin sensitivity, resulting in improvement of glucose intolerance (14, 4, 6).
76 These findings suggest that osteocytes may regulate the function of OCN by
77 orchestrating osteoblast and osteoclast functions. However, it is unknown whether
78 osteocytes are involved in glucose metabolism.

79 AMP-activated protein kinase (AMPK) plays crucial roles as an intracellular
80 energy sensor, and AMPK is closely associated with glucose metabolism (8, 13, 17).
81 Previous studies have shown that AMPK plays roles in both osteoblastogenesis and
82 osteoclastogenesis (7, 9, 10, 11). We previously demonstrated that activation of AMPK
83 stimulates OCN expression as well as osteoblastic differentiation and mineralization via
84 increasing bone morphogenetic protein-2 in MC3T3-E1 cells (9). Moreover, most
85 recently, we showed that AMPK is expressed in osteocytic MLO-Y4 cells, and that
86 AMPK has a protective effect against oxidative stress-induced apoptosis (18) and
87 regulates RANKL expression in the cells (24). A recent study has shown that glucose
88 uptake though glucose transporter 1 (GLUT1) is necessary for osteoblast function (22).
89 Inhibition of GLUT1 activates osteoblast AMPK and subsequently induces proteosomal

Runx2 degradation and decreases OCN and GLUT1 expressions (22). In addition, osteoblast-specific GLUT1 knockout mice showed glucose intolerance by decreasing insulin secretion and sensitivity (22).

The purpose of this study was thus to examine effects of inhibition of glucose uptake by phloretin, a GLUT inhibitor, on expressions of OCN and the molecules involved in bone remodeling such as RANKL, OPG and sclerostin in osteocytic MLO-Y4-A2 cells. We also investigated the role of AMPK in the downstream pathways of glucose uptake in osteocytes.

2. Materials and Methods

2.1. Reagents

Cell culture medium and supplements were purchased from GIBCO-BRL (Rockville, MD). Phloretin, an AMPK inhibitor ara-A, a MAPK/ERK kinase (MEK) inhibitor PD98059, a JNK inhibitor SP600125, a p38 inhibitor SB203580, and anti-β actin antibody were purchased from Sigma–Aldrich (St. Louis, MO). Antibodies against phospho-AMPKα (Thr172), total AMPKα, phospho-ERK1/2, total-ERK1/2, phospho-SAPK/JNK, total-SAPK/JNK, phospho-p38α, total-p38α were purchased from Cell Signaling (Beverly, MA). Anti-RANKL antibody was purchased from Santa Cruz

Biotech (Santa Cruz, CA), and anti-OCN antibody was purchased from Merck Millipore (Bedford, MA).

2.2. Cell cultures

As previously described (19), we used MLO-Y4-A2, a murine long bone-derived osteocytic cell line (12), which was kindly provided by Dr. Y. Kato (Asahi Kasei Medical Corporation, Tokyo, Japan) and Dr. Lynda F. Bonewald (University of Missouri). The cells were cultured on collagen-coated plates in α-minimum essential medium (α-MEM) supplemented with 10% fetal bovine serum and 1% penicillin-streptomycin in 5% CO_2 at 37 °C. The medium was changed twice a week, and the cells were passaged when they were 80% confluence.

2.3. Reverse transcription PCR analysis to identify the expressions of glucose transporter class I subfamily

To investigate the mRNA expressions of GLUT families (GLUT1, GLUT2, GLUT3 and GLUT4) in MLO-Y4-A2 cells, we performed reverse transcription (RT) PCR. Total RNA was extracted from the cultured MLO-Y4-A2 cells using Trizol reagent (Invitrogen, San Diego, CA) according to the manufacturer's recommended

126 protocol. We used 2 μg total RNA for the synthesis of single-stranded cDNA (cDNA
127 synthesis kit; Invitrogen). The primer sequences were: *Glut1* forward,
128 5′-CGTCGTTGGCATCCTTAT-3′; and *Glut1* reverse,
129 5′-TTCTTCAGCACACTCTTGG-3′; *Glut2* forward,
130 5′-TCAGAAGACAAGATCACCGGA-3′; and *Glut2* reverse,
131 5′-GTCGGTGTGACTGTAAGTGGG-3′; *Glut3* forward,
132 5′-ATGGGGACAACGAAGGTGAC-3′; and *Glut3* reverse,
133 5′-CAGGTGCATTGATGACTCCAG-3′; *Glut4* forward,
134 5′-GAGCCTGAATGCTAATGGAG-3′; and *Glut4* reverse,
135 5′-GAGAGAGAGCGTCCAATGTC-3′. The PCR conditions were as follows:
136 denaturation at 94.0°C for 45 s; annealing at 60.0°C for 30 s; and elongation at 72°C for
137 45 sec for 30 cycles. The PCR products were separated by electrophoresis on a 1.8%
138 agarose gel and were visualized using ethidium bromide staining with ultraviolet (UV)
139 light using the Electronic UV trans-illuminator (Toyobo Co. Ltd., Tokyo, Japan).
140
141 2.4. 2-deoxyglucose uptake colorimetric assay
142 Glucose uptake was assayed with a Glucose Uptake Assay Kit (BioVision).
143 The cells were incubated in 96-well plates. After reaching confluent, each well was

144 washed three times with phosphate buffered saline (PBS). The cells were starved for
145 glucose by KRPH buffer (20 mM HEPES, 5 mM KH_2PO_4, 1 mM $MgSO_4$, 1 mM $CaCl_2$,
146 136 mM NaCl and 4.7 mM KCl, pH 7.4) containing 2% BSA for 20 min, and then
147 incubated in KRPH buffer (containing 2% BSA) with phloretin 0 to 100 μM for 20 min.
148 After the buffer was removed, 10 μL of 10 mM 2-deoxyglucose (2-DG) with phloretin
149 0 to 100 μM was added. To examine the reversible effects of phloretin, 2-DG without
150 phloretin was added after 20-min incubation with KRPH buffer with 100μM phloretin.
151 After the cells were further incubated for 20 min, 10μL of Reaction Mix A (assay buffer
152 8μL and enzyme mix 2μL) was added and incubated for 60 min. Extraction buffer 90
153 μL was added and incubated at 85.0°C for 40 min. The plate was cooled on ice for 5
154 min and 12 μL neutralization buffer was added. Thereafter, Reaction Mix B (glutathione
155 reductase 20μL, substrate DTNB 16μL and recycling mix 2μL) 38 μL was added, and
156 the absorbance at 405 nm was measured with a microplate reader. The amount of 2-DG
157 uptake is proportional to the absorbance. The results are expressed as relative to control.
158

159 2.5. Quantification of gene expressions using real-time PCR

160 We used SYBR green chemistry to determine the mRNA levels of *Rankl*, *Opg*,
161 *Sost*, a gene encoding sclerostin, *Ocn* and a housekeeping gene, *36b4*. *36b4* was used to

normalize the differences in the efficiencies of reverse transcription. The primer sequences were: *Rankl* forward, 5′-CACCATCAGCTGAAGATAGT-3′; and *Rankl* reverse, 5′-CCAAGATCTCTAACATGACG-3′; *Opg* forward, 5′-AGCTGCTGAAGCTGTGGAA-3′ and *Opg* reverse, 5′-TGTTCGAGTGGCCGAGAT-3′; *Sost* forward, 5′-GGAATGATGCCACAGAGGTCAT-3′ and *Sost* reverse, 5′-CCCGGTTCATGGTCTGGTT-3′; *Ocn* forward, 5′-TGCTTGTGACGAGCTATCAG-3′ and *Ocn* reverse, 5′-GAGGACAGGGAGGATCAAGT-3′; *36b4* forward, 5'-AAGCGCGTCCTGGCATTGTCT-3' and *36b4* reverse, 5'-CCGCAGGGGCAGCAGTGGT-3'. Real-time PCR was performed using 1 μL of cDNA in a 25 μL reaction volume with ABI PRISM 7000 (Applied Biosystems, Waltham, MA). The double-stranded DNA-specific dye SYBR Green I was incorporated into the PCR buffer provided in the SYBR Green Real-time PCR Master Mix (Toyobo Co. Ltd., Tokyo, Japan) to enable quantitative detection of the PCR product. The PCR conditions were 95°C for 15 min, 40 cycles of denaturation at 94°C for 15 s, and annealing and extension at 60°C for 1 min.

2.6. Western blot analysis

For western blot analysis, the cells were plated in 6-well plates and cultured as described above. After the cells were confluent, they were treated with each agent for up to 72 h. The cells were rinsed with ice-cold PBS and scraped on ice into lysis buffer (BIO-RAD, Hercules, CA) containing 65.8 mM Tris-HCl (pH 6.8), 26.3% (w/v) glycerol, 2.1% SDS, and 0.01% bromophenol blue to which 2-mercaptoethanol was added to achieve a final concentration of 5%. The cell lysates were sonicated for 20 s. The cell lysates were electrophoresed using 10% SDS-PAGE and transferred to a nitrocellulose membrane (BIO-RAD). The blots were blocked with TBS containing 1% Tween 20 (BIO-RAD) and 3% BSA for 1 h at 4°C. Then, the blots were incubated overnight at 4°C with gentle shaking with each primary antibody at a dilution of 1:1000. These blots were extensively washed with TBS containing 1% Tween 20 and were further incubated with a 1:5000 dilution of horseradish peroxidase-coupled IgG of specified animal species (rabbit, goat, or mouse) matched to the primary antibodies in TBS for 30 min at 4°C. The blots were then washed, and the signal was visualized using an enhanced chemiluminescence technique. The bands were quantified with a software ImageJ. The results were described as relative to control.

198 2.7. Statistics

199 Results are expressed as means ± standard error (SE). Statistical evaluations for
200 differences between groups were performed using one-way ANOVA followed by
201 Fisher's protected least significant difference. For all statistical tests, a value of $p < 0.05$
202 was considered a statistically significant difference.

203

204 **3. Results**

205 3.1. Expressions of GLUT and effects of phloretin on glucose uptake in MLO-Y4-A2
206 cells

207 At first, we examined expressions of glucose transporters in MLO-Y4-A2 cells,
208 mouse osteoblastic cell line MC3T3-E1, and mouse bone marrow-derived stromal cell
209 line ST2 by RT-PCR (Fig. 1A). As positive controls, we examined the expression of
210 *Gluts* in mice tissues such as muscle, liver, kidney and brain. *Glut1*, but not *Glut2*, *3* and
211 *4*, was expressed in MLO-Y4-A2, MC3T3-E1 and ST2 cells. In mice tissues, *Glut1* was
212 expressed in muscle, liver, kidney and brain. *Glut2* was expressed in liver and kidney.
213 *Glut3* was expressed in brain. *Glut4* was expressed in muscle and kidney.

214 Next, to confirm the function of GLUT1 in MLO-Y4-A2 cells, we investigated
215 the effect of phloretin on glucose uptake by using 2-deoxyglucose uptake colorimetric

assay. As shown in Fig. 1B, treatments of phloretin (10-100 μM) significantly suppressed 2-DG uptake in MLO-Y4-A2 cells in a dose-dependent manner. Because the effects of 100 μM phloretin was reversible (RC), phloretin did not affect the cells as cellular toxic agent.

3.2. Effects of phloretin on expressions of RANKL, OPG, sclerostin and OCN in MLO-Y4-A2 cells

We investigated effects of phloretin on mRNA expressions of *Rankl*, *Opg*, *Sost* and *Ocn* by real-time PCR in MLO-Y4-A2 cells. As we found that phloretin affected the expression of Rankl and Ocn expression from day 1 to 5 (supplemental figure), we performed the dose-dependent effects of phloretin at day 3 and 5. Phloretin dose-dependently decreased expressions of *Rankl* and *Ocn* mRNA at day 3 and 5 (Fig. 2A and 2D). Phloretin at 100 μM significantly decreased *Opg* mRNA at day3, but no effects of phloretin were found at day 5 (Fig. 2B). The ratio of *Rankl*/*Opg* was dose-dependently decreased (Fig. 2C). The expression of *Sost* mRNA was not affected by Phloretin (Fig. 2E). To confirm the effects of phloretin on *Rankl* and *Ocn* expressions, we performed Western blot analysis. Phloretin significantly decreased protein expressions of RANKL and OCN at day3 (Fig. 2F-I).

234

235 3.3. Roles of AMPK in phloretin-induced decreases in RANKL and OCN expressions in
236 MLO-Y4-A2 cells

237 To examine whether AMPK signal is involved in the effects of phloretin on
238 RANKL and OCN expressions, we investigated effect of phloretin on AMPK
239 phosphorylation. Western blot analysis showed that treatment with phloretin increased
240 phosphorylation of AMPK (Fig. 3A). Furthermore, phloretin significantly
241 phosphorylated AMPK in a dose-dependent manner at 12 h (Fig. 3B and 3D) and 72 h
242 (Fig. 3C and 3E). Real-time PCR showed that an AMPK inhibitor ara-A alone slightly
243 but significantly decreased the expression of *Rankl* mRNA, and co-incubation of ara-A
244 with phloretin additively decreased the *Rankl* mRNA expression (Fig. 3F). In contrast,
245 co-incubation of ara-A with phloretin canceled the phloretin-induced decrease in *Ocn*
246 expression, although ara-A alone had no effect on the expression of *Ocn* mRNA (Fig.
247 3G).

248

249 3.4. Effects of inhibition of MAPK pathways on RANKL and OCN expressions

250 Because AMPK signal was not involved in the phloretin-induced decrease in
251 *Rankl* expression, we examined whether or not MAPK pathways such as ERK1/2, JNK,

and p38 MAPK are associated with the effects of phloretin. Western blot analysis showed that treatment with phloretin (100 μM) clearly decreased phosphorylated ERK1/2 and JNK during 24 h (Fig. 4A). Although phloretin transiently increased phosphorylated p38 MAPK at 1h, phosphorylated p38 MAPK was continuously decreased by phloretin treatment after 3 h (Fig. 4A). Then, we examine the dose-dependent effects of phloretin on MAPK pathways. Phloretin suppressed the phosphorylation of ERK1/2, JNK, and p38 MAPK in a dose-dependent manner at 12 h (Fig. 4B) and 72 h (Fig. 4C). The densities of the bands showed significant decreases in all of ERK1/2, JNK and p38 MAPK (Fig. D-F).

Next, we examined whether inhibition of MAPK pathways affects the expressions of *Rankl* and *Ocn*. Real-time PCR showed that treatments with a MEK inhibitor PD98059 at 20 μM (Fig. 5A), a JNK inhibitor SP600125 at 10 μM (Fig. 5F), or a p38 inhibitor SB203580 at 5 and 10 μM (Fig. 5K) significantly decreased the expression of *Rankl* mRNA. Treatments with PD98059 at 10 and 20 μM (Fig. 5B), or SB203580 at 5 and 10 μM (Fig. 5L) significantly decreased the expression of *Ocn* mRNA although SP600125 did not affect it (Fig. 5G). Western blot analysis showed that PD98059 and SB203580 significantly decreased the protein expressions of RANKL and

OCN (Fig. 5C-E and 5M-O). On the other hand, SP600125 had no effects on protein expressions of RANKL and OCN (Fig. 5H-J).

4. Discussion

Previous studies have shown that bone metabolism is deeply associated with glucose homeostasis. However, there were no studies examining the roles of GLUT and glucose uptake of osteocytes in bone metabolism so far. Further, this is the first study to show the effects of glucose uptake inhibition on OCN in osteocytic cells. The present study showed that GLUT1, but not other GLUT subtypes, is expressed in MLO-Y4-A2 cells, and that inhibition of glucose uptake by phloretin decreased RANKL and OCN expressions. Moreover, phloretin-induced decrease in OCN was mediated by AMPK activation and suppression of MAPK signals, especially ERK1/2 and p38 MAPK. In addition, phloretin-induced decrease in RANKL expression was mediated by suppression of ERK1/2 and p38 MAPK. These results suggest that glucose uptake via GLUT1 is required for the expressions of RANKL and OCN in osteocytes, and that osteocytes may be involved in whole body glucose homeostasis through OCN activation.

Recently, Wei et al. have shown that glucose is the main nutrient for osteoblast function, and that glucose uptake via GLUT1 in osteoblasts is required for maintenance of whole body glucose homeostasis (22). Furthermore, the present study demonstrated that GLUT1 plays important roles in expressions of RANKL and OCN in osteocytes. As osteocytes are derived from differentiated osteoblasts, it is not surprising that glucose uptake is important also for the function of osteocytes. AMPK is known to be an intracellular energy sensor, and AMPK is activated when intracellular AMP/ATP ratio increases (8, 13, 17). Wei et al. showed that inhibition of glucose uptake induced the AMPK-dependent proteosomal degradation of Runx2, a master regulator of osteoblastogenesis, and decreased OCN expression in osteoblasts (22). In this study, AMPK activation by phloretin was involved in the suppression of OCN expression in osteocytic cells. These findings indicate that AMPK plays pivotal roles as a response molecule to decreased glucose uptake in not only osteoblasts but also osteocytes, and that AMPK regulates OCN expression to maintain glucose supply to osteoblastic lineages and glucose homeostasis.

As previous studies showed that osteocytes expressed much higher levels of RANKL and had a great capacity to support osteoclastogenesis (16), osteocytes are considered as the main cells involved in the initiation of bone resorption and remodeling.

304 Although calorie restriction is known to have cardioprotective effects, it induces bone
305 loss, mainly through suppression of bone formation and turnover (20). Because various
306 hormonal signals are altered under calorie restriction condition, the underlying
307 mechanism of effects of calorie restriction on bone metabolism is still unclear. The
308 present study demonstrated that inhibition of glucose uptake decreased the expression of
309 RANKL, but not sclerostin, in MLO-Y4-A2 cells, suggesting that inhibition of glucose
310 supply to osteocytes leads to suppression of bone remodeling. Therefore, decreased
311 glucose uptake into osteocytes may contribute to the calorie restriction-induced low
312 bone resorption by reducing RANKL expression. On the other hand, osteoclasts are
313 reported to be necessary for the function of osteocalcin in glucose metabolism.
314 Treatment with alendronate, a bisphosphonate, showed that the phenotype of glucose
315 abnormality was completely normalized in *Esp*$^{-/-}$ mice, which is a model of gain of
316 OCN bioactivity (4). On the contrary, RANKL treatment induced bone resorption and
317 increased serum level of ucOCN, resulting in less glucose intolerance and less fat mass
318 in WT mice fed a high-fat diet than controls. Taken altogether, these findings indicate
319 that bone resorption is essential to activate osteocalcin and regulate glucose homeostasis
320 by bone. In the present study, inhibition of glucose uptake decreased RANKL
321 expression in MLO-Y4-A2 cells, suggesting that decreased RANKL expression

followed by suppression of bone resorption may lead to reduction in ucOCN production. Therefore, the present study supports the hypothesis that osteocytes may be involved in glucose homeostasis and RANKL may be the more important bone protein involved in it. Further, osteocytes may contribute to keep normal plasma glucose levels by reducing ucOCN secretion when glucose supply is reduced in osteocytes. However, there are not sufficient *in vivo* and human data; thus, further studies are necessary to clarify the hypothesis.

Numerous studies have shown that MAPK signals play important roles in RANKL and OCN expressions in osteoblastic cells. For example, Mine et al. showed that interleukin-33 increased RANKL expression via activation of ERK1/2 and p38 MAPK, but not JNK, in osteoblastic MC3T3-E1 cells (15). Osteoblast-specific p38 knockout mice showed a reduction in trabecular and cortical bone mass due to decreased bone formation (21). In that study, the expressions of type 1 collagen, alkaline phosphatase, and OCN were significantly reduced. In addition, we previously demonstrated that AMPK activation increased phosphorylation of ERK1/2 in MC3T3-E1 cells, and that inhibition of ERK1/2 completely reversed AMPK activation-induced increases in expressions of osteoinductive molecules such as BMP-2 and eNOS, resulting in suppression of osteoblastic differentiation and OCN expression

(9). However, little is known about whether these signals are involved in the function of osteocytes so far. Fontani, et al. recently showed that MAPK signals were involved in RANKL in osteocytes (5). When MLO-Y4 cells were incubated in serum-free medium, RANKL expression was significantly increased. Moreover, incubation with serum-free medium phosphorylated ERK1/2 and JNK signals in MLO-Y4 cells, and the inhibitors of ERK1/2 and JNK significantly reversed the increase in RANKL expression. These findings suggest that ERK1/2 and JNK pathways may be positive regulators of RANKL expression in osteocytes. However, to our knowledge, there were no studies on the roles of p38 MAPK in expression of RANKL in osteocytes. In the present study, inhibition of glucose uptake suppressed ERK1/2, JNK, and p38 MAPK pathways. In addition, a p38 MAPK inhibitor and an ERK inhibitor decreased RANKL and OCN expressions in MLO-Y4-A2 cells. Therefore, the present study for the first time showed that inhibition of glucose uptake by phloretin as well as MAPK inhibition decreases RANKL and OCN expressions in MLO-Y4-A2 cells. However, in this study, phloretin temporally activated p38 MAPK at 1 h and continuously suppressed it after 3 h, although ERK1/2 and JNK were consistently suppressed. Because the roles of transient activation of p38 MAPK is unclear, further studies are needed to clarify it.

As illustrated in Fig. 6, our study showed that inhibition of glucose uptake via GLUT1 by phloretin decreased OCN and RANKL expressions in osteocytic MLO-Y4-A2 cells. Moreover, we demonstrated that AMPK, ERK1/2 and p38 MAPK signals were involved in the phloretin-induced suppression of OCN expression, and that ERK1/2 and p38 MAPK signals might be associated with the phloretin-induced suppression of OCN and RANKL expressions. These findings indicate that glucose uptake is necessary for osteocytes to maintain bone remodeling by RANKL expression, and that osteocytes may regulate the endocrine action of OCN by expressions of OCN and RANKL to keep blood glucose levels.

Disclosures

There are no conflicts of interest.

Acknowledgments

This study was partly supported by a Grant-in-Aid for Scientific Research (C) (15K09433). Authors' roles: Study design and conduct: AT and IK. Performed the experiments and analyzed the data: AT and IK. Contributed equipment/materials: AT, IK, MN, KT and TS. Wrote the paper: AT and IK. Approving final version: All authors. IK

takes responsibility for the integrity of the data analysis. The authors thank Keiko Nagira for technical assistance.

References

1. **Bellido T.** Osteocyte-driven bone remodeling. *Calcified tissue international* 94: 25-34, 2014.

2. **Bonewald LF.** The amazing osteocyte. *Journal of bone and mineral research : the official journal of the American Society for Bone and Mineral Research* 26: 229-238, 2011.

3. **Dallas SL, Prideaux M, and Bonewald LF.** The osteocyte: an endocrine cell ... and more. *Endocrine reviews* 34: 658-690, 2013.

4. **Ferron M, Wei J, Yoshizawa T, Del Fattore A, DePinho RA, Teti A, Ducy P, and Karsenty G.** Insulin signaling in osteoblasts integrates bone remodeling and energy metabolism. *Cell* 142: 296-308, 2010.

5. **Fontani F, Marcucci G, Iantomasi T, Brandi ML, and Vincenzini MT.** Glutathione, N-acetylcysteine and lipoic acid down-regulate starvation-induced apoptosis, RANKL/OPG ratio and sclerostin in osteocytes: involvement of JNK and ERK1/2 signalling. *Calcified tissue international* 96: 335-346, 2015.

6. **Fulzele K, Riddle RC, DiGirolamo DJ, Cao X, Wan C, Chen D, Faugere MC, Aja S, Hussain MA, Bruning JC, and Clemens TL.** Insulin receptor signaling in osteoblasts regulates postnatal bone acquisition and body composition. *Cell* 142: 309-319, 2010.

7. **Jeyabalan J, Shah M, Viollet B, and Chenu C.** AMP-activated protein kinase pathway and bone metabolism. *The Journal of endocrinology* 212: 277-290, 2012.

8. **Kahn BB, Alquier T, Carling D, and Hardie DG.** AMP-activated protein kinase: ancient energy gauge provides clues to modern understanding of metabolism. *Cell metabolism* 1: 15-25, 2005.

9. **Kanazawa I, Yamaguchi T, Yano S, Yamauchi M, and Sugimoto T.** Activation of AMP kinase and inhibition of Rho kinase induce the mineralization of osteoblastic MC3T3-E1 cells through endothelial NOS and BMP-2 expression. *American journal of physiology Endocrinology and metabolism* 296: E139-146, 2009.

10. **Kanazawa I, Yamaguchi T, Yano S, Yamauchi M, and Sugimoto T.** Metformin enhances the differentiation and mineralization of osteoblastic MC3T3-E1 cells via AMP kinase activation as well as eNOS and BMP-2 expression. *Biochemical and biophysical research communications* 375: 414-419, 2008.

11. **Kanazawa I, Yamaguchi T, Yano S, Yamauchi M, Yamamoto M, and Sugimoto T.** Adiponectin and AMP kinase activator stimulate proliferation, differentiation, and mineralization of osteoblastic MC3T3-E1 cells. *BMC cell biology* 8: 51, 2007.

12. **Kato Y, Windle JJ, Koop BA, Mundy GR, and Bonewald LF.** Establishment of an osteocyte-like cell line, MLO-Y4. *Journal of bone and mineral research : the official journal of the American Society for Bone and Mineral Research* 12: 2014-2023, 1997.

13. **Kola B, Boscaro M, Rutter GA, Grossman AB, and Korbonits M.** Expanding role of AMPK in endocrinology. *Trends in endocrinology and metabolism: TEM* 17: 205-215, 2006.

14. **Lee NK, Sowa H, Hinoi E, Ferron M, Ahn JD, Confavreux C, Dacquin R, Mee PJ, McKee MD, Jung DY, Zhang Z, Kim JK, Mauvais-Jarvis F, Ducy P, and Karsenty G.** Endocrine regulation of energy metabolism by the skeleton. *Cell* 130: 456-469, 2007.

15. **Mine Y, Makihira S, Yamaguchi Y, Tanaka H, and Nikawa H.** Involvement of ERK and p38 MAPK pathways on Interleukin-33-induced RANKL expression in osteoblastic cells. *Cell biology international* 38: 655-662, 2014.

16. **Nakashima T, Hayashi M, Fukunaga T, Kurata K, Oh-Hora M, Feng JQ, Bonewald LF, Kodama T, Wutz A, Wagner EF, Penninger JM, and Takayanagi H.** Evidence for osteocyte regulation of bone homeostasis through RANKL expression. *Nature medicine* 17: 1231-1234, 2011.

17. **Ruderman NB, Carling D, Prentki M, and Cacicedo JM.** AMPK, insulin resistance, and the metabolic syndrome. *The Journal of clinical investigation* 123: 2764-2772, 2013.

18. **Takeno A, Kanazawa I, Tanaka K, Notsu M, Yokomoto M, Yamaguchi T, and Sugimoto T.** Activation of AMP-activated protein kinase protects against homocysteine-induced apoptosis of osteocytic MLO-Y4 cells by regulating the expressions of NADPH oxidase 1 (Nox1) and Nox2. *Bone* 77: 135-141, 2015.

19. **Tanaka K, Yamaguchi T, Kanazawa I, and Sugimoto T.** Effects of high glucose and advanced glycation end products on the expressions of sclerostin and RANKL as well as apoptosis in osteocyte-like MLO-Y4-A2 cells. *Biochemical and biophysical research communications* 461: 193-199, 2015.

20. **Tatsumi S, Ito M, Asaba Y, Tsutsumi K, and Ikeda K.** Life-long caloric restriction reveals biphasic and dimorphic effects on bone metabolism in rodents. *Endocrinology* 149: 634-641, 2008.

21. **Thouverey C and Caverzasio J.** The p38alpha MAPK positively regulates osteoblast function and postnatal bone acquisition. *Cellular and molecular life sciences : CMLS* 69: 3115-3125, 2012.

22. **Wei J, Shimazu J, Makinistoglu MP, Maurizi A, Kajimura D, Zong H, Takarada T, Iezaki T, Pessin JE, Hinoi E, and Karsenty G.** Glucose Uptake and Runx2 Synergize to Orchestrate Osteoblast Differentiation and Bone Formation. *Cell* 161: 1576-1591, 2015.

23. **Yasuda H, Shima N, Nakagawa N, Yamaguchi K, Kinoshita M, Mochizuki S, Tomoyasu A, Yano K, Goto M, Murakami A, Tsuda E, Morinaga T, Higashio K, Udagawa N, Takahashi N, Suda T.** Osteoclast differentiation factor is a ligand for osteoprotegerin/osteoclastogenesis-inhibitory factor and is identical to TRANCE/RANKL. *Proc natl Acad Sci USA* 95: 3597-3602, 1998.

24. **Yokomoto-Umakoshi M, Kanazawa I, Takeno A, Tanaka K, Notsu M, and Sugimoto T.** Activation of AMP-activated protein kinase decreases receptor activator of NF-kappaB ligand expression and increases sclerostin expression by inhibiting the mevalonate pathway in osteocytic MLO-Y4 cells. *Biochemical and biophysical research communications* 469: 791-796, 2016.

Figure legends

Figure 1. Expressions of GLUT and inhibition of glucose uptake by phloretin in MLO-Y4-A2 cells

(A) Expressions of GLUT families were investigated by RT-PCR. (B) Glucose uptake was measured by 2-deoxyglucose uptake colorimetric assay. The results are expressed as mean ± SE (n=5). *p<0.05, **p<0.01, ***p<0.001. CR, control of reversible effect of phloretin.

Figure 2. The effects of phloretin on expressions of RANKL, OPG, sclerotsin and OCN in MLO-Y4-A2 cells

(A-E) After reaching confluent, MLO-Y4-A2 cells were incubated with phloretin 0 to 100 μM. The expression levels of *Rankl*, *Opg*, *Sost* and *Ocn* mRNA were examined at day3 and day5 by real-time PCR. The results are expressed as mean ± SE (n≧6). *p<0.05, **p<0.01, ***p<0.001. (F-I) MLO-Y4-A2 cells were treated with phloretin 0 to 100μM for 3 days. Total protein was extracted, and protein expressions of RAKNL

and OCN were examined by Western blot analysis. The results are representative of at least four different experiments (F and G), and quantification of the bands were performed (H and I). The results are expressed as mean ± SE (n≧4). *p<0.05, ***p<0.001. phl; phloretin.

Figure 3. Effects of phloretin on RANKL and OC expressions through AMPK activation in MLO-Y4-A2 cells

(A) After reaching confluent, MLO-Y4-A2 cells were incubated with phloretin 100 μM. The proteins were collected at the indicated time. (B-E) After reaching confluent, MLO-Y4-A2 cells were incubated with phloretin 0 to 100μM. The total proteins were collected at 12 and 72 h. The phosphorylation of AMPK was examined by Western blot analysis. The results of Western blot are representative of at least three different experiments (B and C), and quantification of the bands were performed (D and E). The results are expressed as mean ± SE (n≧3). ***p<0.001. phl; phloretin. (F and G) The cells were treated with phloretin 100 μM and/or an AMPK inhibitor ara-A 0.1 mM for 72 h. *Rankl* and *Ocn* mRNA expressions were examined by real-time PCR. The results are expressed as mean ± SE (n=8). *p<0.05, **p<0.01, ***p<0.001. phl; phloretin.

Figure 4. The effects of phloretin on phosphorylation of MAPKs in MLO-Y4-A2 cells

(A) After reaching confluent, MLO-Y4-A2 cells were incubated with phloretin 100 μM. The proteins were collected at the indicated time. (B-F) After reaching confluent, MLO-Y4-A2 cells were incubated with phloretin 0 to 100μM. The total proteins were extracted at 12 and 72 h, and Western blot analyses were performed. The results are representative of at least four different experiments, and quantification of the bands were performed (D-F). The results are expressed as mean ± SE ($n \geqq 4$). *$p<0.05$, **$p<0.01$, ***$p<0.001$. phl; phloretin.

Figure 5. The effects of MAPK inhibitors on expressions of OCN and RANKL in MLO-Y4-A2 cells

After reaching confluent, MLO-Y4-A2 were treated with a MEK inhibitor PD98059 0 to 20 μM, a JNK inhibitor SP600125 0 to 10 μM, and a p38 inhibitor SB203580 0 to 10 μM for 72 h. The mRNA expressions of *Rankl* (A, F and K) and *Ocn* (B, G and L) were examined by real-time PCR. The results are expressed as mean ± SE ($n \geqq 6$). *$p<0.05$, ***$p<0.001$. The protein expressions of OCN and RANKL were examined by Western

blot. The results are representative of at least three different experiments (C, H and M), and quantification of the bands were performed (D, E, I, J, N, and O).

Figure 6. Schematic illustration of the present study and discussion

GLUT1 is expressed in osteocytic MLO-Y4-A2 cells. Inhibition of glucose uptake by phloretin decreases the expression of RANKL via inhibition of ERK1/2 and p38 MAPK pathways, and decreases the expression of OCN via both activation of AMPK and inhibition of ERK1/2 and p38 MAPK pathways.

Figure 1

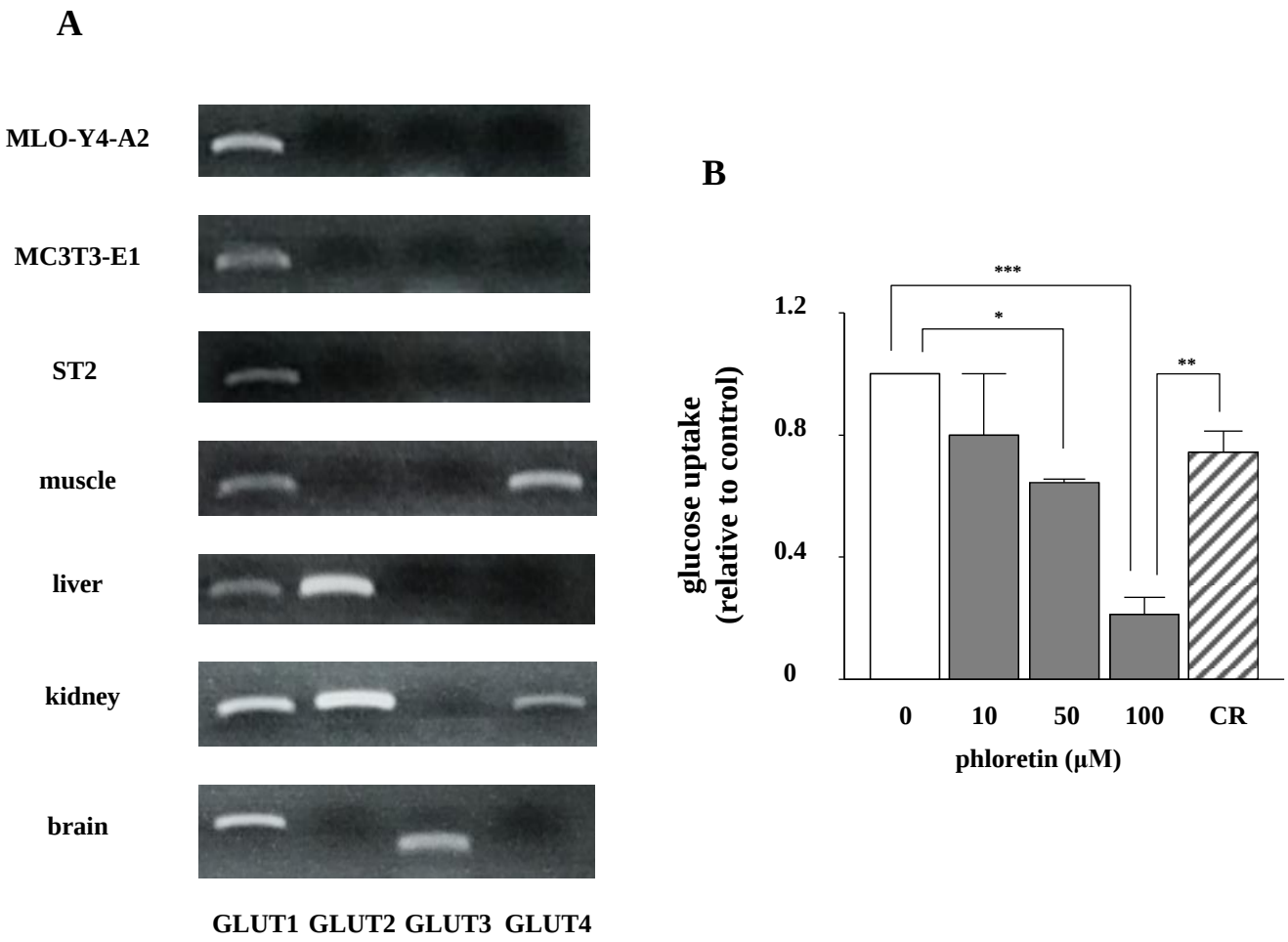
A
MLO-Y4-A2
MC3T3-E1
ST2
muscle
liver
kidney
brain
GLUT1 GLUT2 GLUT3 GLUT4
B
glucose uptake
(relative to control)
1.2
0.8
0.4
0
***
*
**
0
10
50
100
CR
phloretin (μM)

Figure 2

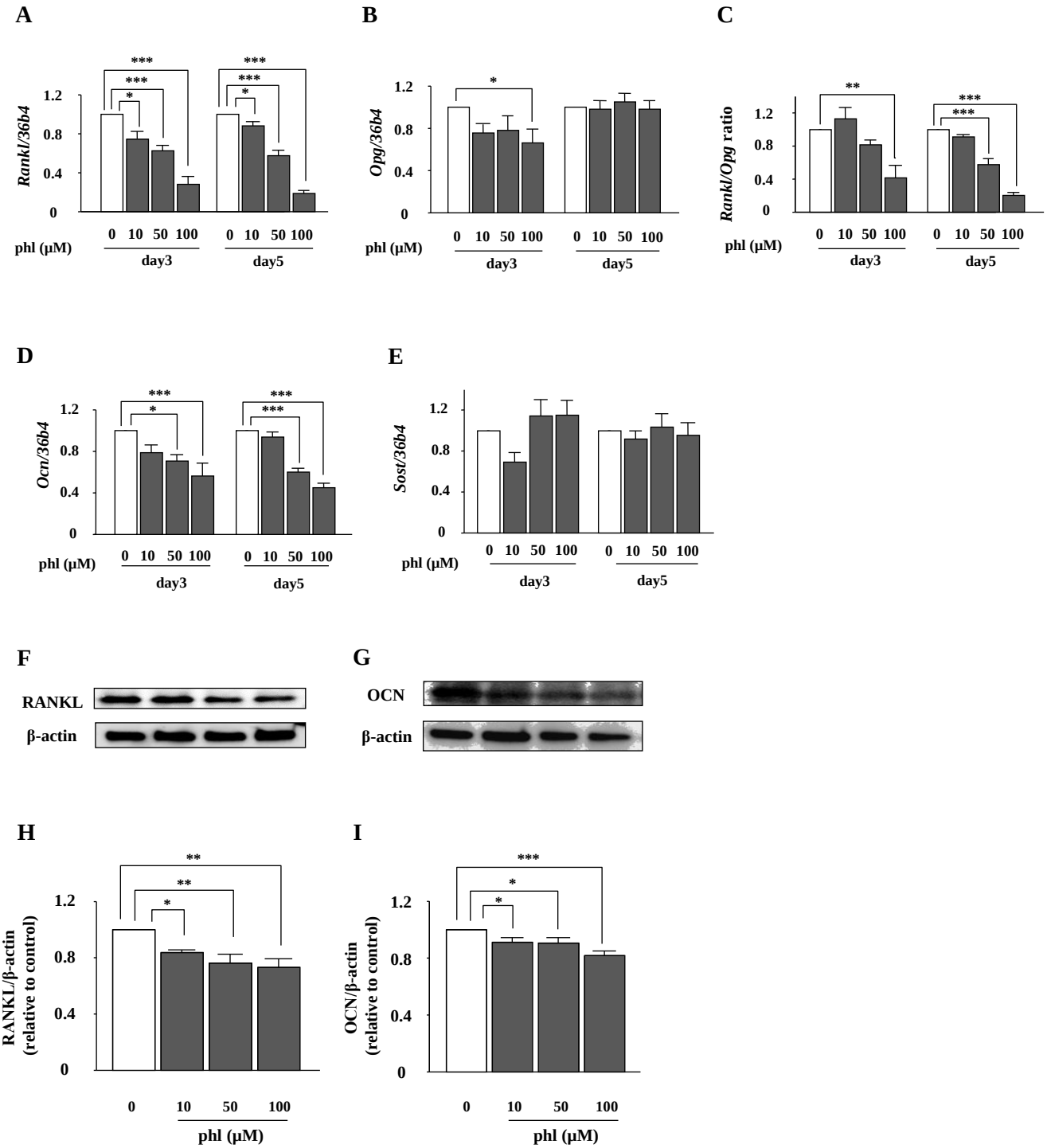
A
B
C
D
E
F
G
H
I
Rankl/36b4
Opg/36b4
Rankl/Opg ratio
Ocn/36b4
Sost/36b4
RANKL
OCN
β-actin
RANKL/β-actin (relative to control)
OCN/β-actin (relative to control)
phl (μM)
0 10 50 100
day3
day5

Figure 3

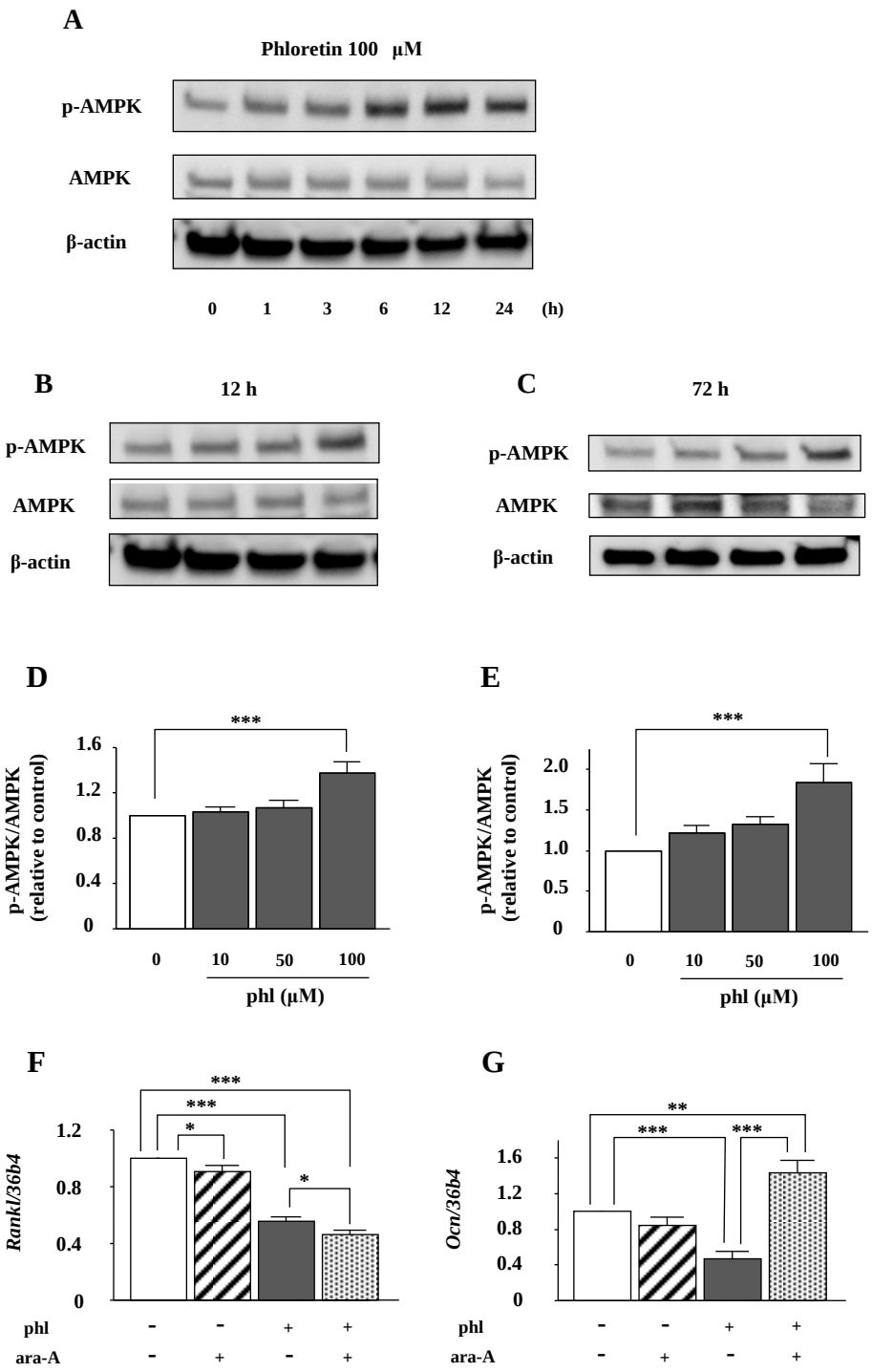
A
Phloretin 100 μM
p-AMPK
AMPK
β-actin
0 1 3 6 12 24 (h)
B
12 h
p-AMPK
AMPK
β-actin
C
72 h
p-AMPK
AMPK
β-actin
D
p-AMPK/AMPK (relative to control)
***
1.6
1.2
0.8
0.4
0
0 10 50 100
phl (μM)
E
p-AMPK/AMPK (relative to control)
***
2.0
1.5
1.0
0.5
0
0 10 50 100
phl (μM)
F
Rankl/36b4
***
***
*
*
1.2
0.8
0.4
0
phl - - + +
ara-A - + - +
G
Ocn/36b4
**
***
***
1.6
1.2
0.8
0.4
0
phl - - + +
ara-A - + - +

Figure 4

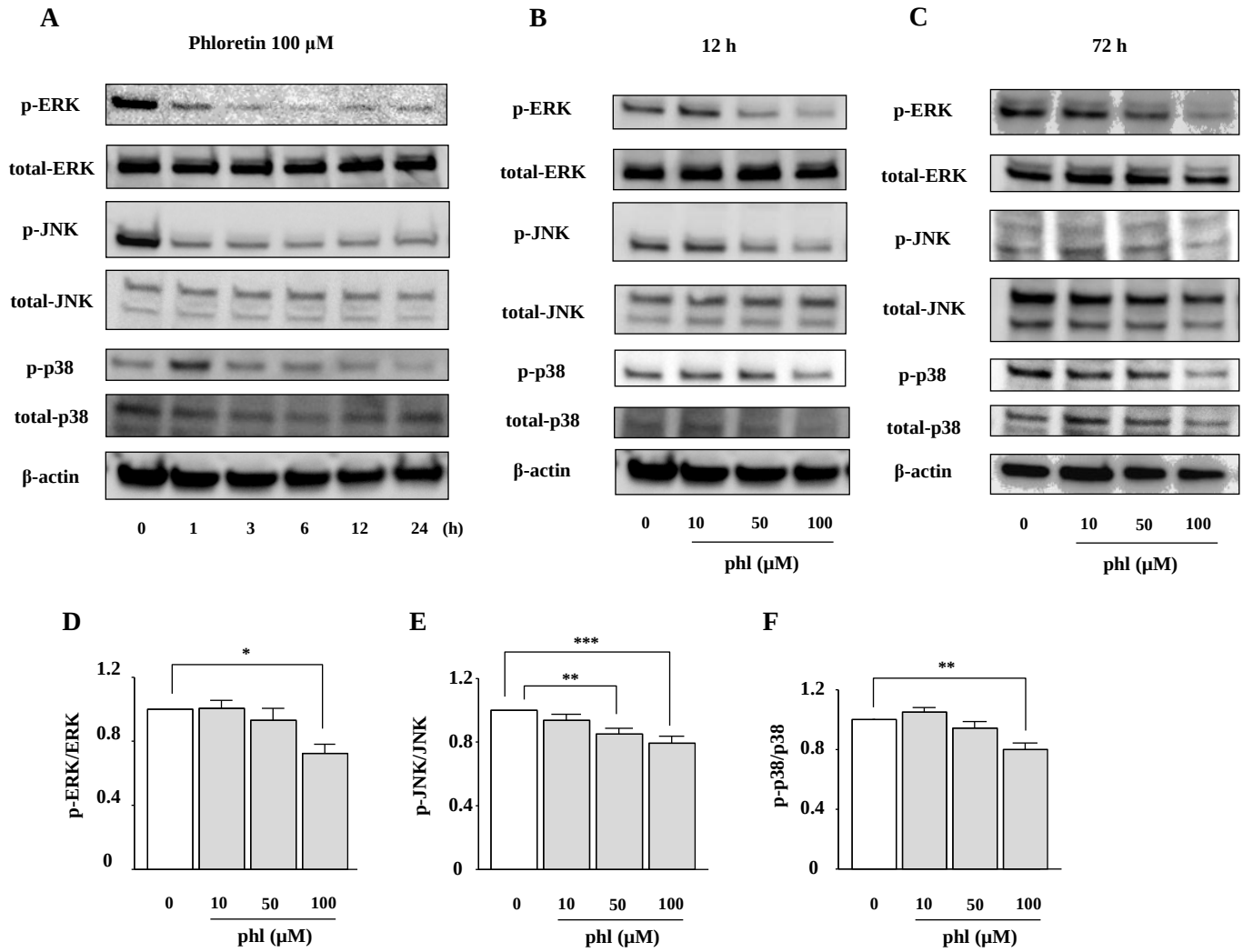
A
Phloretin 100 μM
p-ERK
total-ERK
p-JNK
total-JNK
p-p38
total-p38
β-actin
0 1 3 6 12 24 (h)
B
12 h
0 10 50 100
phl (μM)
C
72 h
0 10 50 100
phl (μM)
D
p-ERK/ERK
1.2
0.8
0.4
0
*
0 10 50 100
phl (μM)
E
p-JNK/JNK
***
**
phl (μM)
F
p-p38/p38
**
phl (μM)

Figure 5

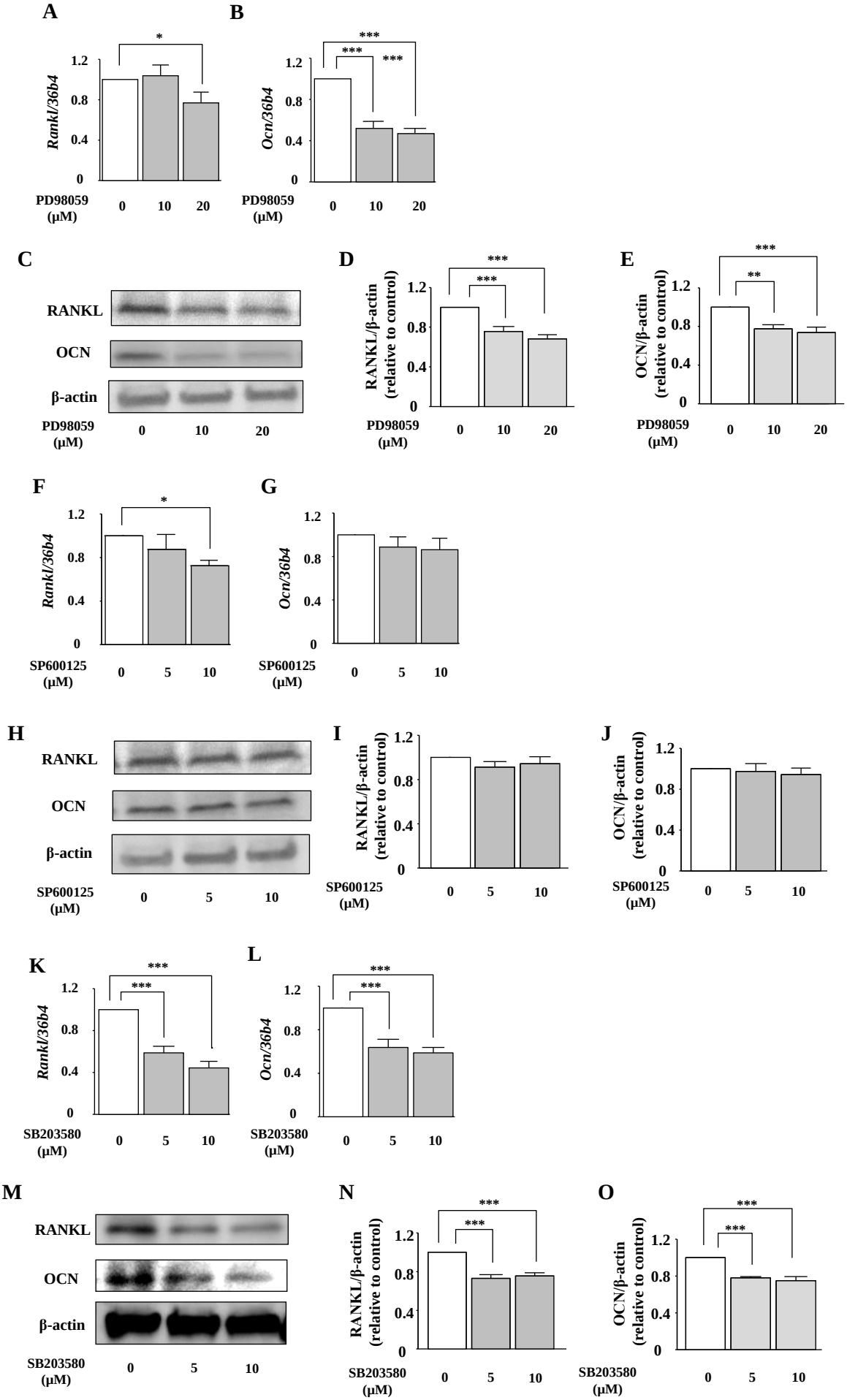
A
B
Rankl/36b4
Ocn/36b4
PD98059 (μM)
0
10
20
C
D
E
RANKL
OCN
β-actin
RANKL/β-actin (relative to control)
OCN/β-actin (relative to control)
F
G
SP600125 (μM)
5
H
I
J
K
L
SB203580 (μM)
M
N
O

Figure 6

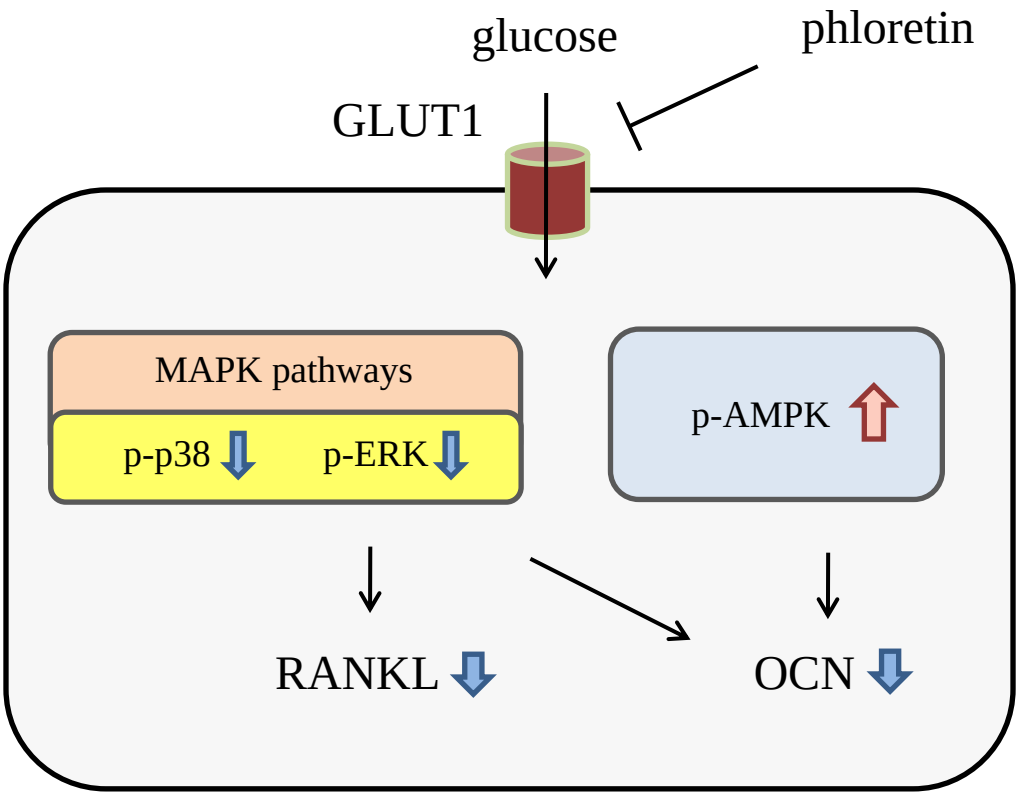
glucose
phloretin
GLUT1
MAPK pathways
p-p38
p-ERK
p-AMPK
RANKL
OCN